

# Time Differences Between Friedel Reflections: Accuracy of Crystal Setting and Requirements on Beam Stability

Yeu-Perng Nieh and John R. Helliwell

Department of Chemistry, University of Manchester, Manchester M13 9PL, UK

(Received 7 December 1994; accepted 31 January 1995)

In synchrotron radiation data collections where the wavelength is carefully set to optimize  $f''$ -derived crystallography intensity differences (Friedel pairs), careful alignment of the crystal is useful to minimize the time differences of stimulation of the reflections in the pairs. This paper quantifies these time differences as a function of crystal misorientation, with typical parameters, using the angular velocity of the crystal. Likewise, the time spent in the diffraction condition is also calculated via the angular reflecting range for a common synchrotron beam geometry. These times offer the user direct insight into the time-dependent aspects of the diffraction measurements. This therefore allows the optimum conditions to be set up so as to extract as accurate anomalous differences as possible in the context of synchrotron radiation beam stability and lifetime.

**Keywords:** crystal setting; Friedel reflections; beam stability.

## 1. Introduction

The monochromatic rotation method is widely used for macromolecular crystallography data collection at synchrotron radiation sources. The requirements on data accuracy can be very demanding for some categories of data collection. One source of error is the variation of the intensity at the crystal sample position. This can occur if there are sudden drops in the beam current, movements of the source position or focal spot drifts from the beamline optics. A particularly exciting application of synchrotron radiation in macromolecular crystallography is that of exploiting the wavelength tunability to vary the anomalous dispersion of specific atoms via the wavelength. The anomalous signal intensities can be small, especially as these techniques are applied to larger protein structures. In chemical crystallography the sites of specific anomalous scatterers can be pinpointed from anomalous differences. Again these signals can be small if a metal has only partially substituted a given site, as can be the case in, for example, metal-substituted aluminophosphates (for a discussion, see Helliwell, Gallois, Kariuki, Kaucic & Helliwell, 1993).

The quality of an  $f''$ -derived signal can be enhanced by careful alignment of the crystal if the crystal has a symmetry mirror plane across the crystal mounting axis. For example, for a  $c^*$  mount  $hkl$  and  $hk\bar{l}$  yield a Friedel intensity difference. The purpose of this paper is to calculate the time difference of stimulation between Friedel mates as a function of crystal misorientation from the perfectly aligned setting. We also give values for the time spent in the reflecting condition for each member of the pair. A 'typical' set of protein crystal sample and beamline conditions are assumed. Our aims are to illustrate to the user the level to which a crystal sample can be usefully aligned, in terms which relate explicitly to the stability with

time, of the beam intensity at the sample. Likewise, the time differences between Friedel mates and the time spent in the reflecting condition will be of interest to accelerator physicists to see how beam instability can surface as errors in the data, thereby constraining the effectiveness of this type of experiment.

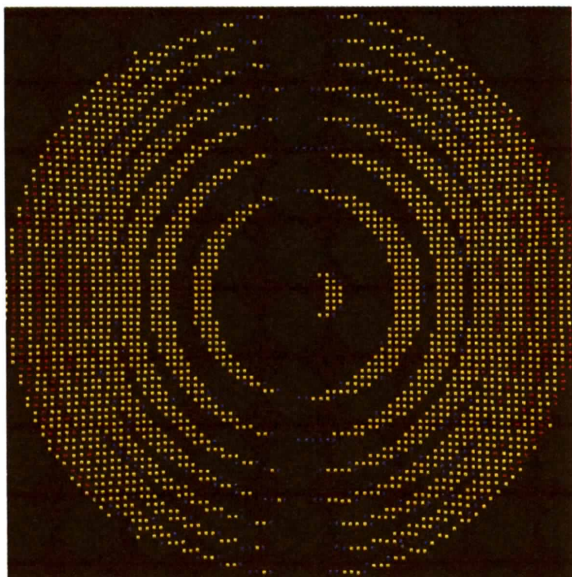
## 2. Diffraction model

In the rotation/oscillation method the protein crystal is rotated over a narrow angular range,  $\Delta\varphi = d_{\min}/a$  where  $d_{\min}$  is the resolution limit and  $a$  is the largest cell parameter of the crystal sample. Typical values are  $d_{\min} = 2.5 \text{ \AA}$ ,  $a = 100 \text{ \AA}$  whereby  $\Delta\varphi = 1.5^\circ$ . A complete data set comprises a large number of such images, contiguous in angle, sufficient to cover an overall angular range, e.g.  $90^\circ$  for an orthorhombic symmetry crystal.

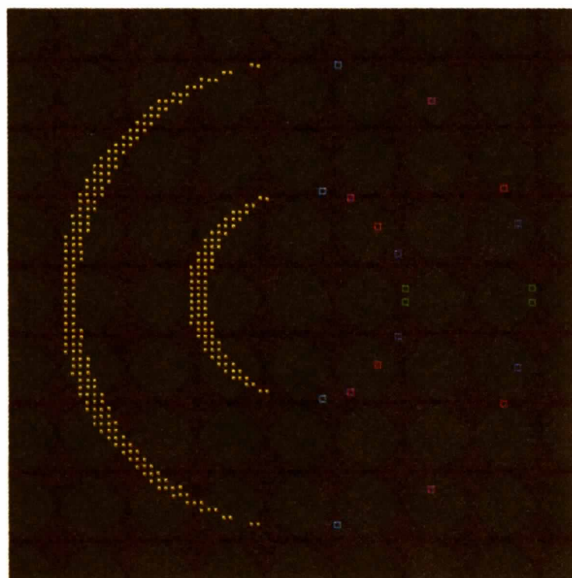
The wavelength may well be tuned in to optimize  $f''$  for an absorption edge, e.g. the Hg  $L_1$  edge at  $0.835 \text{ \AA}$  ( $f'' = 11.9 \text{ e}$  for the free atom), either regularly in a multiple wavelength (MAD) sequence (Hendrickson, 1985) or set there for the whole data collection in a SIROAS data set (Baker *et al.*, 1990).

The exposure time per image (e.g. 40 s is used herein) is often made up of a repeated oscillation (e.g. ten cycles) so that during the oscillation period (4 s) the beam is likely to be stable enough not to affect deleteriously the quality of the diffraction spot intensity measurements. Either way the crystal is rotated during the exposure by a constant angular velocity,  $\omega$ .

For a particular  $hkl$  reflection of interplanar spacing  $d^*$ , the angular reflecting range,  $\varphi_R$ , depends on a number of factors including beam divergence/convergence angles  $\gamma_H$ ,  $\gamma_V$ , spectral spread  $\delta\lambda/\lambda_{\text{conv}}$ , crystal sample mosaicity  $\eta$ ,

**Figure 1**

Rotation image prediction for a  $2^\circ$  angular range for a perfectly set 'typical' protein crystal of  $100 \text{ \AA}$  cell dimensions (orthogonal axes). Fully recorded reflections in yellow, partially recorded reflections in blue and spatial overlaps in red (since  $2^\circ > d_{\min}/a$ , see §2). The rotation axis is in the vertical direction. The simulation was performed using the program *OSCGEN* (Wonacott, Dockerill & Brick, 1980) and also the *XDL-VIEW* routines of the current version of the Daresbury *LAUE* software.

**Figure 2**

Two lunes selected from Fig. 1 at 6 and  $3 \text{ \AA}$  resolution, respectively, on the left, and individual Friedel pairs from these lunes highlighted, on the right. The colour code for these pairs is (a) at  $6 \text{ \AA}$ , green =  $-1, 17, \pm 1$ ; blue =  $1, 16, \pm 6$ ; red =  $-1, 13, \pm 10$ ; violet =  $-1, 9, \pm 14$ ; turquoise =  $-1, 5, \pm 15$ ; and (b) at  $3 \text{ \AA}$ , green =  $-5, 34, \pm 1$ ; blue =  $-5, 32, \pm 10$ ; red =  $-5, 30, \pm 15$ ; violet =  $-5, 20, \pm 27$ ; turquoise =  $-5, 7, \pm 32$ . The rotation axis is in the vertical direction. Fully recorded reflections only.

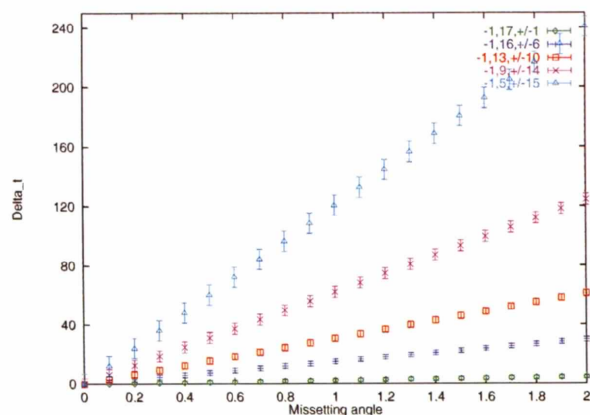
and varies for different spots according to the position in reciprocal space ( $\zeta, \theta$ ), according to the equation

$$\varphi_R = [L^2(\zeta\gamma_H)^2 + \gamma_V^2]^{1/2} + 2\varepsilon_s L \quad (1)$$

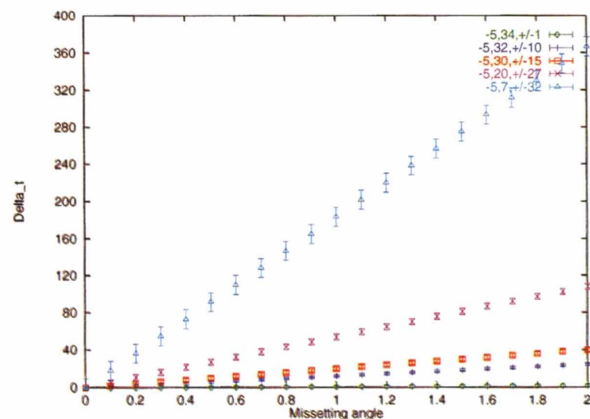
where  $\varepsilon_s = (d^* \cos \theta_{hkl}/2)[\eta + (\delta\lambda/\lambda)_{\text{conv}} \tan \theta_{hkl}]$  and  $L = \text{Lorentz factor} = 1/(\sin^2 2\theta - \zeta^2)^{1/2}$  (Greenough & Helliwell, 1982). This assumes that for a triangular monochromator it is operating at the Guinier position ( $\delta\lambda/\lambda_{\text{corr}} = 0$ ). The time spent in the reflecting condition for a given spot is therefore  $\varphi_R/\omega$ .

The actual mean angle that a reflection is stimulated at, with respect to a zero reference setting, is given by

$$\varphi = 2 \tan^{-1} \left[ \frac{2y_0 \pm (4y_0^2 + 4x_0^2 - d^{*4})^{1/2}}{(d^{*2} - 2x_0)} \right] \quad (2)$$



(a)



(b)

**Figure 3**

The time differences for the partners of the Friedel pairs [highlighted in Fig. 2 (right)] as derived from application of equation (2) to both members of each pair. (a)  $6 \text{ \AA}$  group, (b)  $3 \text{ \AA}$  group. The error bars represent the time spent in the reflecting condition in each case derived from equation (1); note that the error bar is the same for each member of the pair (see Table 1).

where  $x_0$  and  $y_0$  are coordinates in reciprocal space perpendicular to the rotation axis (Arndt & Wonacott, 1977). Hence, the actual moment in time that this reflection is stimulated with respect to the start of the scan can be calculated. From this, and a similar calculation for its Friedel mate (e.g.  $hk\bar{l}$ ), the time difference between the two reflections can be derived. Two sets of such pairs are taken as examples at two resolution values (6 and 3 Å) and covering a variety of  $\zeta$  values (Figs. 1 and 2).

### 3. Results and discussion

The time differences between Friedel pairs plotted *versus* a misorientation angle are shown in Fig. 3 within the two different resolution groups. The misorientation angle chosen is about the vertical axis so as to affect immediately the alignment about the central mirror plane in the image shown in Figs. 1 and 2. Various trends are discernible. The Friedel pairs closest to the mirror plane are least affected so that the time difference between these remains small. As  $\zeta$  increases though, those reflections further away from the mirror plane are vulnerable. These time differences for the 6 Å group, are 30 s or so, even for an angle-setting error as small as  $0.2^\circ$ . These time differences are exacerbated for the 3 Å group, where the equivalent time value corresponding to crystal mis-setting of  $0.2^\circ$  is 40 s. The 'error bars' shown on the plot are the values for the time spent by each partner in the reflecting condition derived from the appropriate  $\varphi_R$  values [equation (1), see Table 1].

These calculations all assume a single rotation of the crystal to make up an image. An image made up of  $N$  oscillations would have the time differences reduced by  $1/N$ . However, the oscillation strategy would then be at the expense of the duty cycle because during the reverse periods the X-ray shutter is usually closed, so as to avoid angular backlash effects of the crystal rotation motor. It is therefore more effective to use a lower number of (slower) sweeps.

Another strategy, besides that of oscillating the crystal  $N$  times to deal with beam decay, is to make the exposure time at each step through a scan proportional to the dose at the sample (Bartunik, Clout & Robrahn, 1981). This dose is measured *via* a beam intensity monitor placed between the end of the collimator and the crystal. This is well suited to the case where there is a smooth intensity decay and the reflections are not very sharp in angular reflecting range. However, at shorter wavelengths the size of the signal can be very weak, and hence inaccurate, owing to the limited space available in the collimated beam path.

Another adverse effect of crystal mis-setting is that as  $\zeta$  increases the partners of the Friedel pair can be on successive images rather than within the same image (Table 2). Hence, errors in scaling of reflection intensities on different images are introduced. In the Weissenberg image-plate method employed at synchrotron radiation sources (Sakabe, 1991), larger  $\varphi$  sweeps per image are used (e.g.  $10\text{--}20^\circ$ ) and reasonable crystal alignment is employed, so that this error condition is not going to occur. Indeed, the

**Table 1**  
Rocking width in time,  $t$ .

$h$	$k$	$l$	$\zeta$ (r.l.u.)	$\varphi_R$ ( $^\circ$ )	Rocking time (s)
(a) Selection of reflections at $\sim 6$ Å as a function of $\zeta$					
-1	17	1	0.009	0.063	1.25
-1	17	-1	-0.009	0.063	1.25
-1	16	6	0.055	0.079	1.58
-1	16	-6	-0.055	0.079	1.58
-1	13	10	0.092	0.111	2.22
-1	13	-10	-0.092	0.111	2.22
-1	9	14	0.129	0.187	3.75
-1	9	-14	-0.129	0.187	3.75
-1	5	15	0.138	0.341	6.82
-1	5	-15	-0.138	0.341	6.82
(b) Selection of reflections at $\sim 3$ Å as a function of $\zeta$					
-5	34	1	0.009	0.062	1.25
-5	34	-1	-0.009	0.062	1.25
-5	32	10	0.092	0.075	1.50
-5	32	-10	-0.092	0.075	1.50
-5	30	15	0.138	0.088	1.77
-5	30	-15	-0.138	0.088	1.77
-5	20	27	0.248	0.167	3.33
-5	20	-27	-0.248	0.167	3.33
-5	7	32	0.294	0.512	10.23
-5	7	-32	-0.294	0.512	10.23

Notes: The calculation of  $\varphi_R$  assumes values for the synchrotron beam parameters used in equation (1) of  $\gamma_H = 1$  mrad,  $\gamma_V = 0.2$  mrad,  $(\delta\lambda/\lambda)_{\text{conv}} = 0.0005$ ,  $\lambda = 0.92$  Å. Also, the crystal sample mosaic spread was  $0.05^\circ$ . The angular velocity of the crystal assumed was  $20\text{ s deg}^{-1}$ .

**Table 2**  
Mis-setting angles ( $^\circ$ ) beyond which reflections are outside the oscillation range of one image.

$h$	$k$	$l$	$\Delta\varphi_y$	$h$	$k$	$l$	$\Delta\varphi_y$
(a) At $\sim 6$ Å				(b) At $\sim 3$ Å			
-1	17	1	>2	-5	34	1	>2
-1	17	-1	>2	-5	34	-1	>2
-1	16	6	>2	-5	32	10	>2
-1	16	-6	>2	-5	32	-10	1.647
-1	13	10	1.209	-5	30	15	>2
-1	13	-10	1.388	-5	30	-15	1.111
-1	9	14	0.142	-5	20	27	0.820
-1	9	-14	1.142	-5	20	-27	0.665
-1	5	15	0.074	-5	7	32	0.341
-1	5	-15	0.591	-5	7	-32	0.091

careful setting of the crystal needed in that method satisfies the conditions advocated here. However, the disadvantages of the image plate in terms of low sensitivity to weak signals and poor duty cycle/offline nature (Lewis, 1994) are being overcome by CCDs (Allinson, 1994) used in oscillation/rotation designs rather than Weissenberg (detector translation) schemes. Hence, it is useful to emphasize careful crystal alignment, for MAD and SIROAS, in the oscillation method too.

Careful and rapid crystal alignment is increasingly easily performed as synchrotron radiation instruments for macromolecular crystallography now tend to have a three-circle goniostat included in the hutch, e.g. ESRF beamline 19 (Thompson, 1993; Deacon *et al.*, 1995).

#### 4. Conclusions

For monochromatic data collection runs in macromolecular crystallography where  $f''$  anomalous differences are to be measured, alignment of the crystal to exploit a mirror plane, *e.g.* using a three-circle goniostat, can greatly reduce the time difference of stimulation of the partners in the Friedel pair. This can therefore reduce the impact of time-dependent variations in the intensity of the sample on the measured anomalous difference. The times given here are also a guide to accelerator physicists and beamline optics specialists of the time-dependent aspects of this kind of experiment, and reflect the continued interest of users in realizing long lifetimes of the circulating current and good beam position stability. Sudden jumps in beam intensity at the sample are particularly damaging to data quality in general and the quality of anomalous differences in particular.

We are grateful to Drs S. J. Harrop and J. Raftery for discussions.

#### References

- Allinson, N. M. (1994). *J. Synchrotron Rad.* **1**, 54–62.
- Arndt, U. W. & Wonacott, A. J. (1977). *The Rotation Method in Crystallography*, pp. 80. Amsterdam: Elsevier.
- Baker, P. H., Farrants, G. W., Stillman, T. J., Britton, K. L., Helliwell, J. R. & Rice, D. W. (1990). *Acta Cryst.* **A46**, 721–725.
- Bartunik, H. D., Clout, P. N. & Robrahn, B. (1981). *J. Appl. Cryst.* **14**, 134–136.
- Deacon, A., Habash, J., Harrop, S. J., Helliwell, J. R., Hunter, W. N., Leonard, G. A., Peterson, M., Kalb (Gilboa), A. J., Allinson, N. M., Castelli, C., Moon, K., McSweeney, S., Gonzalez, A., Thompson, A. W., Ealick, S., Szebenyi, D. M. & Walter, R. (1995). *Rev. Sci. Instrum.* In the press.
- Greenhough, T. J. & Helliwell, J. R. (1982). *J. Appl. Cryst.* **15**, 493–508.
- Helliwell, M., Gallois, B., Kariuki, B., Kaucic, V. & Helliwell, J. R. (1993). *Acta Cryst.* **B49**, 420–428.
- Hendrickson, W. A. (1985). *Trans. Am. Crystallogr. Assoc.* **21**, 11–21.
- Lewis, R. (1994). *J. Synchrotron Rad.* **1**, 43–53.
- Sakabe, N. (1991). *Nucl. Instrum. Methods*, **A303**, 448–463.
- Thompson, A. W. (1993). *ESRF Beamline Handbook*, p. 59. ESRF, Grenoble, France.
- Wonacott, A. J., Dockerill, S. & Brick, P. (1980). *MOSFLM Program*. Unpublished notes.